The stem cell marker *Prom1* promotes axon regeneration by down-regulating cholesterol synthesis via Smad signaling

Jinyoung Lee[a,1], Jung Eun Shin[b,1], Bohm Lee[a], Hyemin Kim[a], Yewon Jeon[a], Seung Hyun Ahn[a], Sung Wook Chi[a], and Yongcheol Cho[a,2]

[a]Department of Life Sciences, Korea University, 02841 Seoul, Republic of Korea; and [b]Department of Molecular Neuroscience, Dong-A University College of Medicine, 49201 Busan, Republic of Korea

Edited by Reinhard Jahn, Max Planck Institute for Biophysical Chemistry, Goettingen, Germany, and approved May 15, 2020 (received for review November 26, 2019)

Axon regeneration is regulated by a neuron-intrinsic transcriptional program that is suppressed during development but that can be reactivated following peripheral nerve injury. Here we identify *Prom1*, which encodes the stem cell marker prominin-1, as a regulator of the axon regeneration program. *Prom1* expression is developmentally down-regulated, and the genetic deletion of *Prom1* in mice inhibits axon regeneration in dorsal root ganglion (DRG) cultures and in the sciatic nerve, revealing the neuronal role of *Prom1* in injury-induced regeneration. Elevating prominin-1 levels in cultured DRG neurons or in mice via adeno-associated virus-mediated gene delivery enhances axon regeneration in vitro and in vivo, allowing outgrowth on an inhibitory substrate. *Prom1* overexpression induces the consistent down-regulation of cholesterol metabolism-associated genes and a reduction in cellular cholesterol levels in a Smad pathway-dependent manner, which promotes axonal regrowth. We find that prominin-1 interacts with the type I TGF-β receptor ALK4, and that they synergistically induce phosphorylation of Smad2. These results suggest that *Prom1* and cholesterol metabolism pathways are possible therapeutic targets for the promotion of neural recovery after injury.

Prominin-1 | sciatic nerve injury | cholesterol metabolism | Smad | Activin

The regenerative potential of injured axons can be promoted by manipulating the expression of specific genes within neurons. Modulating the expression of regeneration-associated genes (RAGs) has become an attractive strategy for the development of therapeutic applications that restore neuronal connectivity (1, 2). Comparative analysis of transcriptome has revealed highly promising targets for manipulation to effectively enhance axon regeneration (3–6). This approach has also led to the identification of signaling pathways regulating axon regeneration, such as the MAPK, JAK/STAT, BMP/Smad, and PTEN/mTOR pathways (7–12). However, it remains unclear which cellular physiological mechanisms, such as metabolic processes, protein secretion, and cytoskeletal remodeling, are affected by the manipulation of these signaling pathways for the purposes of regenerative potentiation. Thus, identification of the specific biological processes is required to develop clinically applicable methods.

Prominin-1, also known as CD133, is a pentaspan membrane glycoprotein encoded by *Prom1* that has been identified in human hematopoietic stem cells and mouse neuroepithelium (13–15). It has been demonstrated that the genetic deletion of *Prom1* causes significant neural defects, including retinal degeneration (16, 17), a reduced number of neurons in the brain (18), and walking problems (19). Collectively, these previous findings indicate that prominin-1 may be involved in neural integrity (20). However, whether prominin-1, the protein encoded by *Prom1*, can regulate the intrinsic ability of damaged neurons to regenerate axons has not yet been tested.

Axon regeneration in the central nervous system (CNS) is challenging because of the inhibitory environment in the damaged neural tissue, which hinders axonal growth (21, 22). In addition, the neurons in the CNS cannot activate the regenerative program, leading to unrecoverable defects in neural function after injury (23). In contrast, the neurons in the peripheral nervous system (PNS) can usually recover their original function after injury based on their robust regenerative potential (24). It has also been reported that engineered PNS neurons can overcome the growth-stunting effects of inhibitory molecules produced by injured CNS tissue (25). Research into transcriptomic mechanisms for regeneration has revealed that injury to peripheral neurons activates intrinsic signals that enhance the regenerative process, which is known as the preconditioning effect (26–30). In this regard, signaling pathways have been suggested as possible targets for the promotion of axonal regeneration in vivo (23, 31, 32). However, the search continues for effective target molecules for manipulation to improve axon reextension in injured neural tissue (33).

In the present study, we identified the stemness-associated gene *Prom1* as a positive regulator of axon regeneration and the preconditioning effect. *Prom1* expression in dorsal root ganglia (DRG) is developmentally down-regulated, and elevating its expression levels enhances the intrinsic regenerative potential of injured neurons. We report that *Prom1* overexpression

Significance

This work presents a concept for promoting the neuronal regenerative potential by engineering the expression of a stem cell marker, *Prom1*. We identify *Prom1* as a developmentally down-regulated neuronal intrinsic factor of axon regeneration. Replenishing *Prom1* expression amplifies the axonal regenerative potential by transcriptionally inhibiting cholesterol metabolism via Smad-dependent signaling. We provide evidence that a reduction in cholesterol synthesis empowers neuronal regrowth capacity. This work suggests that Food and Drug Administration-approved cholesterol-lowering drugs are potential candidates for neuroregenerative medicine.

Author contributions: J.L., J.E.S., and Y.C. designed research; J.L., J.E.S., B.L., H.K., Y.J., S.H.A., S.W.C., and Y.C. performed research; J.L., J.E.S., B.L., H.K., Y.J., S.H.A., S.W.C., and Y.C. analyzed data; and J.E.S. and Y.C. wrote the paper.

The authors declare no competing interest.

This article is a PNAS Direct Submission.

Data deposition: The data reported in this paper have been deposited in the Gene Expression Omnibus (GEO) database, https://www.ncbi.nlm.nih.gov/geo (accession no. GSE147936).

[1]J.L. and J.E.S. contributed equally to this work.

[2]To whom correspondence may be addressed. Email: ycho77@korea.ac.kr.

This article contains supporting information online at https://www.pnas.org/lookup/suppl/doi:10.1073/pnas.1920829117/-/DCSupplemental.

First published June 17, 2020.

induces transcriptomic regulation of a distinct set of genes associated with cholesterol metabolism via Smad signaling, which leads to improved axon regeneration, and present the *Prom1*-dependent pathway as a target of therapeutic methods for enhancing neural repair.

Results

***Prom1* Expression Is Developmentally Down-Regulated in DRG Neurons.** The ability to regenerate axons deteriorates as neurons mature, which is consistent with the idea that developmentally down-regulated genes may contribute to the limited regenerative potential in adult neurons (20, 34). We hypothesized that stemness-regulating genes, which have reduced levels in adult neurons, might play an important role in the regenerative program. The transcriptome in DRG in the early stages of development is distinct from that in mature DRG (6), suggesting that comparative analysis could be used to identify the molecular determinants regulating the developmental stages of neurons.

Based on a list of genes that have been reported to be differentially expressed in the early or late developmental stages (6), we searched for known stem cell marker genes (35). We found that the expression of a specific set of stem cell marker genes is negatively regulated across the developmental stages of DRG neurons (Fig. 1*A*). Except for *Prom1*, most of these factors are known to regulate gene expression during neuronal differentiation. The expression levels of the stem cell marker genes were further analyzed and plotted with the expression levels in cultured DRG neurons (at days in vitro [DIV] 7) reported in our previous study to confirm neuronal expression (27) (Fig. 1*B*). A series of comparative analyses between the independent datasets revealed that *Prom1* is substantially down-regulated as the neurons mature. More importantly, *Prom1* mRNA is detected from cultured DRG neurons at DIV7 (closed circles in Fig. 1*B*). In contrast, the transcripts of the other genes, such as *Sox9*, *Msi1*, and *Sox2*, were not expressed (open circles in Fig. 1*B*). qPCR analysis confirmed significantly lower *Prom1* mRNA expression levels in DRG dissected from 8-wk-old adult mice compared with DRG dissected from mouse embryos (embryonic day [E] 12.5), unlike other tested genes involved in neuronal development, such as *Zbp1*, *Shh*, and *Fgf1* (36–38) (Fig. 1*C*). Collectively, these results suggest that *Prom1* is developmentally down-regulated and is potentially responsible for the developmental decline in the regenerative response in injured PNS neurons.

We then examined the expression of prominin-1, the protein encoded by *Prom1*. Prominin-1 is known to be preferentially localized in the plasma membrane and also often in cellular protrusions, such as microvilli, cilia, and filopodia (15, 39–43), but its cellular localization in neuronal tissue has not been clearly determined. We detected prominin-1 in the neuronal cell bodies (white arrowhead) and in the βIII-tubulin-negative filamentous structure (red arrow) adjacent to the soma (Fig. 1*D*). Neither type of immunostaining signal was observed in the DRG tissue from *Prom1* constitutive knockout (KO) mice, confirming that both staining patterns are prominin-1–specific (Fig. 1*E*). We next investigated the identity of the prominin-1–positive filamentous structure. Based on the morphology and location of the structure, we tested the colocalization of prominin-1 with the vascular marker CD31 and F-actin. We found that phalloidin and CD31 immunoreactivity showed a partial overlap with the prominin-1–positive structure (Fig. 1*E* and *SI Appendix*, Fig. S1*A*), consistent with the vascular expression of prominin-1 (44–46). Collectively, these results demonstrate that prominin-1 is expressed in the neuronal cell bodies and vascular structure in the DRG.

We also assessed neuronal prominin-1 expression levels before and after nerve injury. Twenty-four hours after introducing a crush injury to the sciatic nerve, where the DRG neurons project their peripheral axons, the immunostaining intensity against prominin-1 was reduced specifically in the βIII-tubulin–positive neuronal cell bodies but not in the vascular structure

A

Gene	Involved in regulation of gene expression	Normalized mean expression value (Tedeschi et al., 2016)		
		E12.5	E17.5	log $_2$FC
Sox9	Yes	2201.5	55.5	-5.31
Msi1	Yes	392.1	15.6	-4.65
Nes	Yes	15213.1	1271.8	-3.58
Prom1	Unknown	595.8	52.5	-3.50
Sox2	Yes	2893.2	283.1	-3.35
Gli3	Yes	1914.3	201.1	-3.25
Gli2	Yes	975.1	138.6	-2.81
Mcm2	Yes	1486.4	239.0	-2.64
Notch1	Yes	3365.7	810.7	-2.05
Pcna	Yes	1891.3	480.2	-1.98

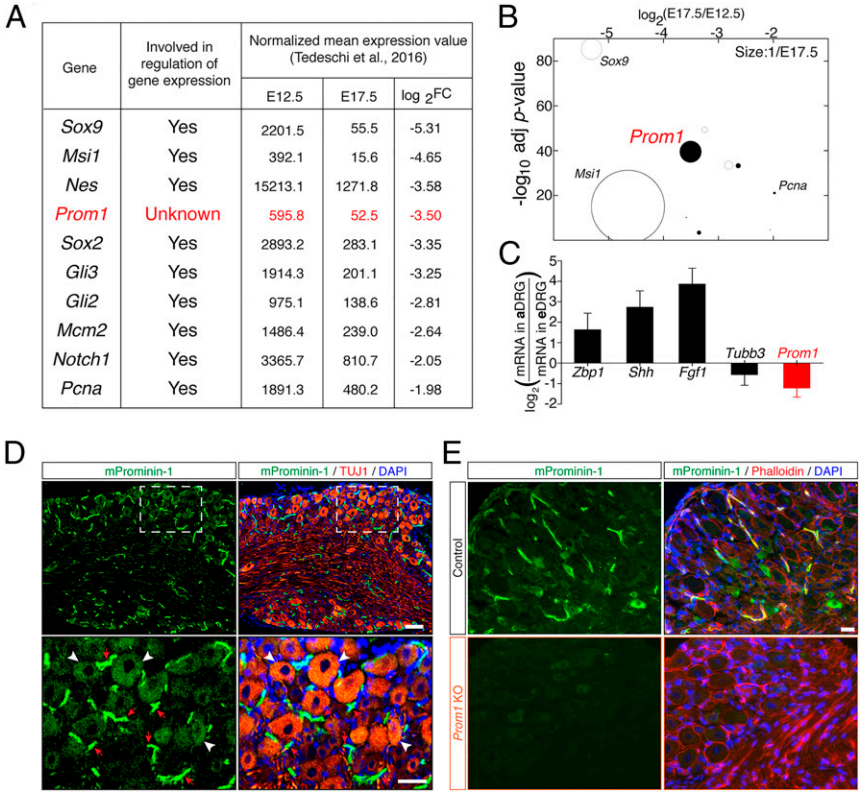

Fig. 1. *Prom1* is a neuronally expressed and developmentally down-regulated stem cell marker in DRG. (*A*) Table of expression values for stem cell markers at different developmental stages in mouse embryos. The data were extracted and adopted from the original GEO accession no. GSE66128 (6). (*B*) 3D bubble plot of the log2 FC in the expression values at E17.5/E12.5 (*x*-axis), the −log10-adjusted *P* value for differential gene expression analysis from the original reference GSE66128 (*y*-axis), and the inverse of the expression values at E17.5 (the diameter). The open and closed circles indicate genes that have negative or positive detection values, respectively, analyzed and compared with the results from the original reference (27). (*C*) The relative mRNA levels from mouse adult DRG (aDRG) or E12.5 embryonic DRG (eDRG) tissue. Data are mean ± SEM (*D*) A representative section of adult mouse DRG tissue immunostained with anti-mouse prominin-1 (mProminin-1) and anti-βIII tubulin (TUJ1) antibodies. Prominin-1 was immunodetected in neuronal cell bodies (white arrowheads) and in filamentous structures (red arrows). (Scale bars: 100 μm; 20 μm for the magnified image [dotted box].) (*E*) Representative cryosection of adult mouse DRG tissue collected from control and *Prom1*-KO mice immunostained with an mProminin-1 antibody and counterstained with phalloidin for F-actin and DAPI for nuclei; refer to *SI Appendix*, Fig. S1.

(*SI Appendix*, Fig. S1*B*). Therefore, neuronal prominin-1 expression displays a decline in response to nerve injury.

***Prom1* Is Required for Axon Regeneration.** The neuronal function of *Prom1* has been unclear (47–50). To understand the role of *Prom1* in mature neurons in adult mice, we investigated the role of *Prom1* in the activation of the axonal regeneration program in the PNS after injury, using a *Prom1* constitutive KO mouse line (51). First, the axonal regeneration of the DRG neurons was assessed in vivo by introducing a crush injury (Fig. 2*A*). Immunostaining for SCG10, a marker for regenerating axons, showed robust axonal regrowth in the control mice, with SCG10 immunoreactivity normalized to the crush site referred to as the regeneration index. We found that *Prom1* deficiency resulted in inefficient axon regeneration in the crushed sciatic nerves (Fig. 2 *A*–*C*). Moreover, the sciatic nerve injury in *Prom1* KO mice did not potentiate axonal regrowth in the cultured DRG neurons as effectively as in the WT controls, indicating that *Prom1* is required for the full induction of preconditioning effect by nerve injury (Fig. 2 *D* and *E*). The DRG neurons cultured from the prelesioned adult control mice showed robust axon regeneration, with a 3.6-fold increase in the average axon length due to preconditioning potentiation, consistent with previous reports (11) (Fig. 2*F*). However, the DRG neurons from the prelesioned *Prom1* KO mice displayed partial impairment in promoting axonal regrowth, with the preconditioning effect reduced by 30% compared with the control neurons (Fig. 2*F*). Notably, the loss of *Prom1* expression did not affect axonal growth in the naïve contralateral DRG (Fig. 2 *E* and *F*), indicating that *Prom1* is required for injury-induced activation of the regenerative program rather than initial axon extension after injury.

We next assessed the contribution of *Prom1* in regulating the regenerative potential in relation to environmental effects. We used a culture dish coated in chondroitin sulfate proteoglycans (CSPGs) for the neuronal cultures to produce conditions physiologically unfavorable for axon growth, which is one of the molecular barriers inhibiting axon regeneration in damaged CNS tissue. Neurons potentiated by a preconditioning injury exhibit only limited axon elongation under growth-inhibitory conditions (52–56). As expected, we found that the preconditioned neurons obtained from the adult control mice at 72 h after nerve injury do not efficiently regenerate axons on the CSPG substrate, with the average axon length reaching only 48.5% of that seen in the permissive environment (Fig. 2 *G* and *H*). CSPG treatment did not inhibit regeneration further in the *Prom1* KO neurons, indicating that *Prom1* deficiency has a robust inhibitory effect. Collectively, these results demonstrate that *Prom1* is required for activation of the neuronal regenerative program, which induces axonal regrowth after injury.

***Prom1* Is a Neuronal Intrinsic Factor Regulating Axon Regeneration.** Axon regeneration is regulated by both intrinsic and extrinsic neuronal factors in the nervous system (56). To determine whether *Prom1* functions as an intrinsic or an extrinsic regulator of the regenerative program, we tested whether *Prom1* is required for the preconditioning effect induced by an in vitro axon injury to the cultured adult DRG neurons. By trypsinizing and replating the cultured neurons, the grown axons were injured and removed in vitro, so that neuronal injury-responsive signal transduction was initiated without environmental influences. The WT DRG neurons were able to shift their physiological condition from a resting state to a regenerative state following the replating injury, which resulted in a 2.6-fold increase in the average axon length compared with the control neurons with no replating injury (Fig. 3 *A* and *B*), as reported previously (57, 58). In contrast, *Prom1* KO neurons displayed significant defects in axonal growth, as shown by the shorter axon lengths (Fig. 3*A*). *Prom1* KO DRG neurons enhanced axonal growth by an only

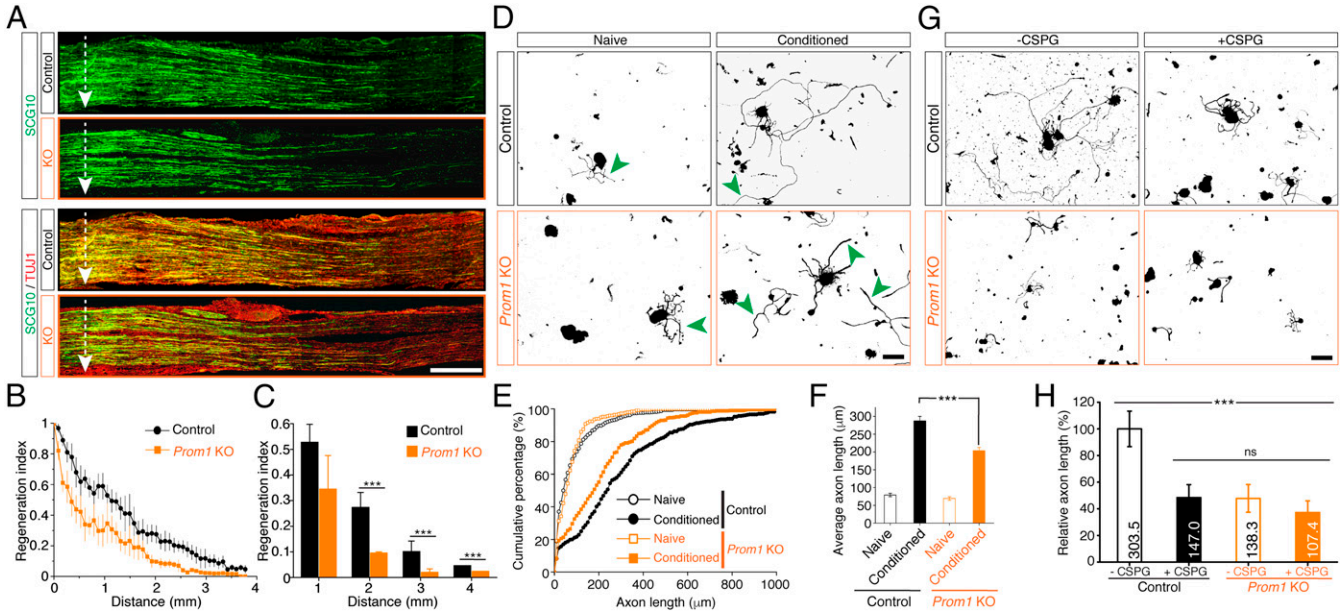

Fig. 2. *Prom1* is required for axon regeneration. (*A*) In vivo axon regeneration assays of adult mouse sciatic nerves dissected at 3 d after injury. Shown are representative images of the longitudinal sections immunostained with TUJ1 and anti-SCG10 antibodies. The white arrows indicate the injury sites where the nerves were crushed using forceps. (Scale bar: 500 μm.) (*B* and *C*) In vivo regeneration index calculated using the SCG10 intensity measured at the injured site to the distal part, normalized to the intensity at the injured site. Data are mean ± SEM. (*D*) DRG neurons were dissected from 12-wk-old control or *Prom1*-KO mice with (i.e., conditioned) or without (i.e., naïve) preconditioning potentiation via sciatic nerve injury, cultured for 12 h and stained with an anti-βIII tubulin antibody. (Scale bar, 100 μm.) (*E* and *F*) Cumulative percentage of the longest axon length per DRG neuron (*E*) and average length of the longest axons per neuron (*F*) from the results in *D*. Data are mean ± SEM. (*G*) Conditioned DRG neurons were dissected from 12-wk-old control or *Prom1*-KO mice, incubated for 12 h on culture dishes coated with CSPG (+) or without CSPG (–), and stained with an anti-βIII tubulin antibody. (Scale bar: 100 μm.) (*H*) Relative axon length of the DRG neurons from *G*. Data are mean ± SEM. Refer to *SI Appendix*, Fig. S10.

1.8-fold increase in average axon length following the replating injury (Fig. 3*B*). Compared with the replated WT controls, *Prom1* deficiency caused a 28% reduction in the axon length, demonstrating the requirement of neuronal *Prom1* in fully activating the regenerative program. Furthermore, knocking down *Prom1* in vitro reduced the axonal regeneration of the embryonic DRG neurons cultured from WT mice (Fig. 3 *C*–*F*). These results show that *Prom1* functions as a neuronal intrinsic factor responsible for regulating axonal growth and regenerative potential after injury.

Neuronal Overexpression of *Prom1* Enhances Axon Regeneration. Because we found that *Prom1* is an intrinsic regulator of axon regeneration, we next asked whether manipulating the neuronal expression levels of *Prom1* could enhance the regenerative potential. Human *PROM1* was overexpressed via lentiviral transduction in the embryonic DRG neurons (Fig. 3*G*). We found that the *PROM1*-overexpressing DRG neurons displayed robust axonal regrowth on reassessment after replating on the permissive substrate without CSPGs (Fig. 3*H*). The *PROM1*-overexpressing DRG neurons showed regenerating axons with an average length significantly longer than the control (46% increase, control vs. *Prom1* overexpression; Fig. 3*I*).

To test whether *Prom1* overexpression activates the regenerative potential even on the growth-inhibitory, nonpermissive substrate, the DRG neurons were replated on CSPG-coated dishes. In the control neurons, the CSPG-mediated inhibition led to a 20% reduction in the average axon length (Fig. 3 *H* and *I*). The percent reduction in average axon length appeared comparable in *PROM1*-overexpressing neurons (20% decrease by +CSPG) (Fig. 3*I*); however, *PROM1*-overexpressing neurons were able to extend their axons on the CSPG-coated substrate with an average length even longer than that in the control neurons grown on the permissive substrate without CSPGs (Fig. 3 *I* and *J*). Prominin-1 is a transmembrane protein, but its receptor function has not been studied extensively. To test whether *Prom1* function in the regulation of regeneration involves its potential role as a receptor, we used the synthetic peptide LS-7. LS-7 has been reported to bind to the extracellular region of prominin-1 and inhibit its cellular function, consistent with its action as a potential receptor (59). We confirmed that LS-7 has an affinity for prominin-1 in vitro and that the application of LS-7 to DRG neurons removed the effect of *PROM1* overexpression in promoting axon regrowth, supporting its function through the extracellular domain (*SI Appendix*, Fig. S2). These results suggest that *Prom1*-regulated physiology is a potential target for promoting the intrinsic regenerative capacity, which may allow the extension of injured axons on regeneration-unfavorable conditions.

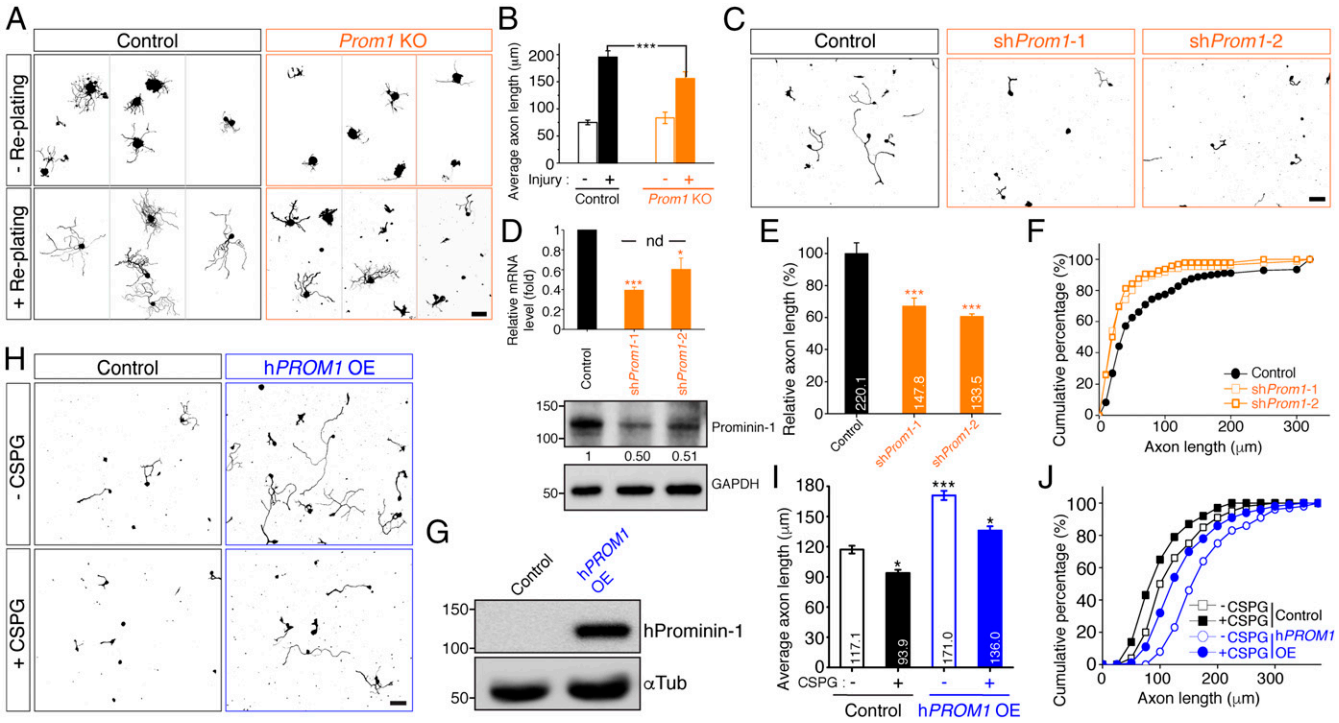

Fig. 3. *Prom1* is a neuronal intrinsic regulator of axon regeneration. (*A*) DRG neurons were dissected from 12-wk-old control or *Prom1*-KO mice without a preconditioning nerve injury. The naïve (−replating) or injured (+replating) neurons were fixed and stained with an anti-βIII tubulin antibody. (Scale bar: 100 μm.) (*B*) Average length of the longest axon per neuron from *A*. Data are mean ± SEM. (*C*) *Prom1*-shRNA or control shRNA was delivered into cultured embryonic DRG neurons via lentivirus infection at DIV2. A neuronal injury was introduced by replating at DIV5. The replated neurons were incubated for 12 h and then fixed and stained with an anti-βIII tubulin antibody. (Scale bar: 100 μm.) Two different shRNA sequences targeting *Prom1*—(sh*Prom1*-1 and sh*Prom1*-2)—were used. (*D*, *Upper*) RT-qPCR analysis of relative mRNA level of *Prom1* from cultures transduced with control or individual *Prom1* knockdown lentivirus (*shProm1*-1 and sh*Prom1*-2). Data are mean ± SEM from three replicates. (*D*, *Lower*) Western blot analysis of prominin-1 from total protein lysates. The numbers indicate the relative intensity obtained from ImageStudio (LI-COR). (*E*) Average axon length of neurons in *C*. Data are mean ± SEM. (*F*) Cumulative percentage of the axon length per neuron from the results shown in *C*. (*G*) Western blot analysis of human *PROM1* (h*PROM1*)-overexpression in embryonic DRG culture. Anti-human prominin-1 antibody was used to confirm overexpression of human *PROM1* delivered by lentiviral infection in *H*. (*H*) Control or *PROM1*-overexpressing DRG neurons replated on regeneration-favorable (−CSPG) or inhibitory (+CSPG) substrates. A control or *PROM1*-overexpressing lentivirus was used to infect mouse embryonic DRG neurons at DIV2. The neurons were replated on culture dishes coated with (+CSPG) or without CSPGs (-CSPG) at DIV5 and fixed and stained with an anti-βIII tubulin antibody at 12 h after replating. (Scale bar: 100 μm.) (*I*) The average length of axons from *H*. Data are mean ± SEM. (*J*) Cumulative percentage of the axon length per neuron from the results shown in *H*. Refer to *SI Appendix*, Figs. S2 and S10.

***Prom1* Gene Delivery Enhances the Neuronal Regenerative Potential In Vivo.** The observation of the enhanced axon regeneration in cultured embryonic DRG neurons encouraged us to test whether manipulating *Prom1* expression in vivo also promotes the regenerative response. Because *Prom1* is developmentally downregulated in DRG neurons, we first tested whether the transduction of an adeno-associated virus (AAV) can successfully overexpress *PROM1* in adults. An AAV expressing GFP or human *PROM1* was delivered into neonatal mice via a facial vein injection, followed by confirmation of expression by Western blot analysis and immunocytochemistry at 12 wk after the injection (Fig. 4 *A*–*D*). The Western blot analysis revealed that the systematic delivery of AAV-GFP and AAV-h*PROM1* successfully maintained the high expression levels of GFP (Fig. 4*C*) and prominin-1 (Fig. 4*B*) in adult DRG tissue. We further confirmed that prominin-1 was successfully overexpressed in the soma of DRG neurons from AAV-injected mice using an anti-mouse prominin-1 antibody, consistent with its neuronal role (Fig. 4*D*).

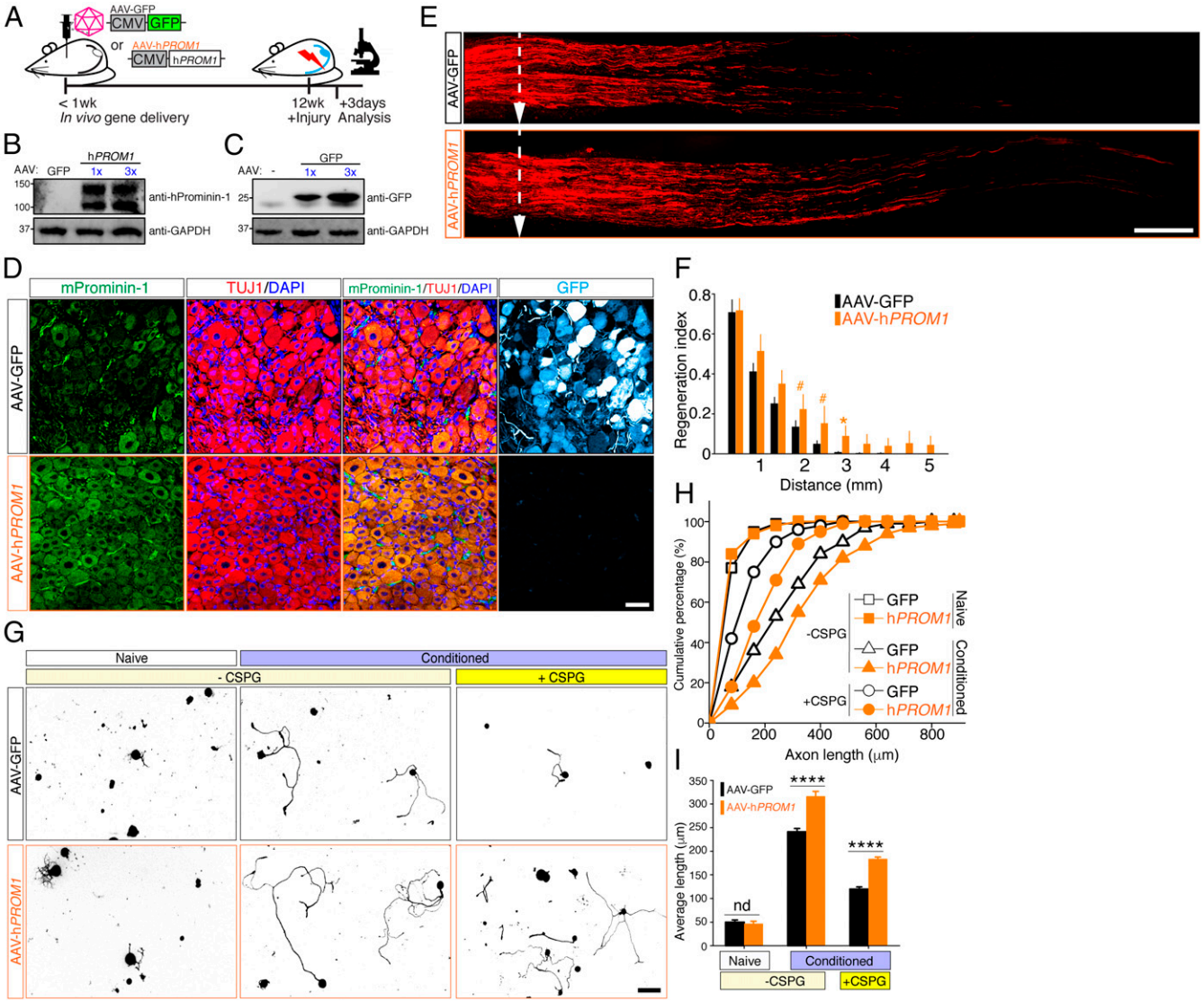

Fig. 4. *Prom1* overexpression promotes axon regeneration in vivo. (*A*) Schematic illustration of in vivo gene delivery to overexpress human *PROM1* in adult mice. AAV-GFP–expressing GFP protein served as a control. Here "wk" denotes week of the experimental schedule. (*B* and *C*) Western blot analysis of human prominin-1 or GFP protein from DRG tissue dissected from AAV-injected mice. "3×" denotes DRG lysates prepared from mice injected with a threefold volume of the viral preparation. Anti-human prominin-1 antibody (hProminin-1) was used for detecting overexpressed human prominin-1 (*B*). GFP expression from control mice was confirmed by Western blot analysis with anti-GFP antibody (*C*). (*D*) Representative images of DRG sections from 12-wk-old AAV-GFP– or AAV-h*PROM1*–injected mice. An anti-mouse prominin-1 antibody that immunoreacts to formaldehyde-fixed mouse and human prominin-1 was used. (*E*) Representative longitudinal sections of mouse sciatic nerves immunostained with an anti-SCG10 antibody. The nerves were dissected at 12 wk after GFP- or human *PROM1*-AAV injection. Axonal injury was introduced at 3 d before dissection by crushing the sciatic nerve. The dotted white arrow indicates the injury site. (Scale bar: 500 μm.) (*F*) The regenerating axons were assessed using SCG10 immunostaining intensity, which was continuously measured along sections from the injury site to the distal part of the injured sciatic nerves collected from the GFP- or h*PROM1*-AAV-injected mice. The average regeneration index was plotted from the injury site (0 mm) to the distal end (6 mm). Data are mean ± SEM. (*G*) At 12 wk after AAV injection, the DRG neurons were prepared from mice expressing GFP or human *PROM1* with (conditioned) or without (naïve) sciatic nerve injury to introduce the preconditioning effect. The neurons were cultured on a regeneration-favorable (–CSPG) or regeneration-inhibitory substrate (+CSPG). The DRG neurons were fixed at 12 h after plating and stained with an anti-βIII tubulin antibody. (Scale bar: 100 μm.) (*H* and *I*) Cumulative percentage of the length of the longest regenerating axon per DRG neuron (*H*) and the average length of the longest axon per neuron (*I*). Data are mean ± SEM. Refer to *SI Appendix*, Fig. S10.

We investigated the effect of *PROM1* expression using the sciatic nerve regeneration model and found that AAV-h*PROM1*–injected mice displayed longer regenerating axons in the injured sciatic nerves compared with the control nerves (Fig. 4*E*). SCG10 immunoreactivity was apparent even in the far distal region of the crushed nerves, 5 mm away from the injury site (Fig. 4 *E* and *F*).

We next investigated the regenerative potential of DRG neurons in *PROM1*-overexpressing mice. We found that the adult DRG neurons dissected from GFP- or *PROM1*-overexpressing mice without preconditioning potentiation grew only short neurites (Fig. 4*G*), indicating that the persistent expression of *PROM1* alone is not sufficient to ready the neuronal state for activation of the regeneration program. Most of the naïve DRG neurons (>90%) had axons shorter than 100 μm (Fig. 4*H*). The average length of the naïve neurons from both groups was approximately 50 μm, with no statistically significant difference (Fig. 4*I*). In contrast, with preconditioning lesions, the DRG neurons cultured from the *PROM1*-overexpressing mice displayed longer axons on the permissive substrate compared with controls (Fig. 4*G*). More than 50% of the neurons had axons longer than 200 μm (Fig. 4*H*). In addition, the average axon length in *PROM1*-overexpressing neurons was 31% greater than the average in the control neurons (Fig. 4*I*). These results suggest that the persistent expression of *Prom1* in vivo augments the regenerative potential of the neurons, after activated by injury signals.

We also investigated whether the *Prom1*-mediated potentiation sufficiently increases the growth capacity of injured neurons to regenerate their axons in a growth-inhibitory environment characteristic of damaged CNS tissue, using the in vitro assay. In control mice injected with AAV-GFP, the effects of preconditioning nerve injury on promoting axon outgrowth was reduced on the CSPG-coated substrate, with the average axon length decreased to one-half of that observed under permissive (-CSPG) conditions (Fig. 4 *G–I*). However, the neurons from *PROM1*-overexpressing mice showed effective axonal regrowth on the inhibitory substrate and displayed a 53% increase in average axon length compared with the control neurons. They also reached 76% of the average axon length of the control neurons under permissive conditions, suggesting that the inhibition of growth by CSPGs can be partially compensated for by replenishing *Prom1* expression (Fig. 4*I*). Thus, *PROM1*-overexpressing DRG neurons retain the regenerative potential to allow axonal reconstruction even on an inhibitory substrate.

***Prom1* Overexpression Inhibits the Expression of Cholesterol Metabolic Genes.** The transcriptional transition from a naïve to a regenerative state is required for functional recovery after nerve injury (4, 5, 21, 23, 24, 26, 28–33, 56, 60, 61). Thus, we investigated the transcriptional profiles responsible for *PROM1* expression-mediated regenerative potentiation (62). Using cultured embryonic DRG neurons transduced with lentivirus, we found that a total of 94 and 84 genes were significantly down- or up-regulated, respectively, by human *PROM1* overexpression (the red triangles in Fig. 5*A*, referred to as *PROM1*-differentially expressed genes [DEGs] hereinafter; Dataset S1). The expression levels of these DEGs are known to be enriched in the nervous system (Fig. 5*B*), suggesting that *Prom1* has a specific role in direct or indirect regulation of transcription in the nervous system, although no evidence has been reported to date.

To identify the shared transcriptomic landscape of the *Prom1*-dependent pathway and injury signals, we compared the *PROM1*-DEGs with injury-responsive genes (IRGs) identified in our previous study (3). We found that a set of genes was commonly regulated by *PROM1* overexpression and the nerve injury, with 90 of the 663 genes regulated by *PROM1* overexpression ($P < 0.05$) detected on the IRG list. While this was significantly greater overlap than would be expected by chance (1.5-fold overenrichment; $P = 1.01E-04$ via hypergeometric testing), the expression fold changes (FCs) due to *PROM1* and the nerve injury exhibited only a weak positive correlation (Pearson's $r = 0.24$; Fig. 5*C* and Dataset S2). These results indicate that transcriptional regulation by *PROM1* overexpression does not significantly mimic the injury-induced activation of the regeneration program. Furthermore, *PROM1*-regulated gene expression showed only a modest overlap with transcriptional regulation by the key regulator of regeneration, DLK (3).

We previously reported injury-responsive transcriptomes with DLK dependency at different time points after sciatic nerve injury (3). While *PROM1* appeared responsible for regulating the expression of a subset of DLK-dependent genes (1.8-fold overenrichment; $P = 3.14E-04$ via hypergeometric testing), the expression FCs due to *PROM1* overexpression and DLK deficiency had only a mild negative correlation (Pearson's $r = -0.39$; Fig. 5*D* and Dataset S2). These results indicate that *PROM1* does not strongly regulate the endogenous transcriptional program that is promoted by injury in a DLK-dependent manner. Rather, *PROM1* is likely to induce a distinct transcriptional response that can augment the regenerative outcome of the preconditioning injury. Consistently, we found that the *PROM1*-DEGs were distinct from RAGs. Of the 37 RAGs defined by Ma and Willis (63) and Finelli et al. (64), only *Fos* and *Onecut1* were identified in *PROM1*-DEG analysis (Fig. 5 *C* and *D*). These results suggest that *PROM1* overexpression may regulate specific cellular physiological mechanisms that have not previously been recognized as an important pathway regulating regeneration (24).

To identify the *Prom1*-regulated cellular mechanisms contributing to regenerative potentiation, we first analyzed the biological functions of the *PROM1*-DEGs using Gene Ontology (GO) term analysis. The results revealed that *PROM1* regulates specific genes with related functions (65) because the biological processes related to *PROM1*-DEG were specifically enriched with annotations associated with lipid metabolism, such as cholesterol/isoprenoid synthesis and lipid/steroid metabolism (Fig. 5*E*). Because this GO analysis revealed a biological process that differs from previously recognized injury-responsive signaling, we cross-compared the GO analysis results with our previously published IRG dataset and a dataset of developmentally regulated DEGs (3, 6). Interestingly, the GO biological process terms associated with sterol and lipid metabolism were specific to the *PROM1*-DEGs and were not overrepresented in the IRGs or developmentally regulated DEGs (Fig. 5*F*). In contrast, biological processes such as transcriptional regulation, cell proliferation, and development were shared by the other datasets. Therefore, the sterol and lipid metabolism pathways are the biological processes specifically regulated by *PROM1* overexpression. Surprisingly, we also found that the *PROM1*-DEGs annotated with significantly enriched lipid metabolic pathways were consistently down-regulated when *PROM1* was overexpressed (Fig. 5*G*). *PROM1* overexpression significantly reduced the expression of all 11 *PROM1*-DEGs annotated by cholesterol biosynthesis, steroid biosynthesis, and steroid metabolism (Fig. 5*H*), suggesting that *PROM1* overexpression may inhibit cholesterol synthesis. Consistent with specific roles of the cholesterol metabolism genes in regulating *Prom1*-mediated regenerative responses, expression levels of the 11 *PROM1*-DEGs were not significantly altered after nerve injury in adult DRG tissue according to our previously published RNA-seq dataset (3). However, from an independent RNA-seq study using sciatic nerve segments, we found that all 11 genes were down-regulated in the proximal segment of transected sciatic nerves at 24 h after injury (*SI Appendix*, Fig. S3*A*) (4). Moreover, qPCR analysis showed that the 11 genes were also consistently down-regulated by axotomy in cultured embryonic DRG neurons (*SI Appendix*, Fig. S3*B*), supporting the involvement of the cholesterol metabolism pathway in certain injury conditions.

We subsequently investigated the functional associations among the 11 *PROM1*-DEGs by STRING analysis and found

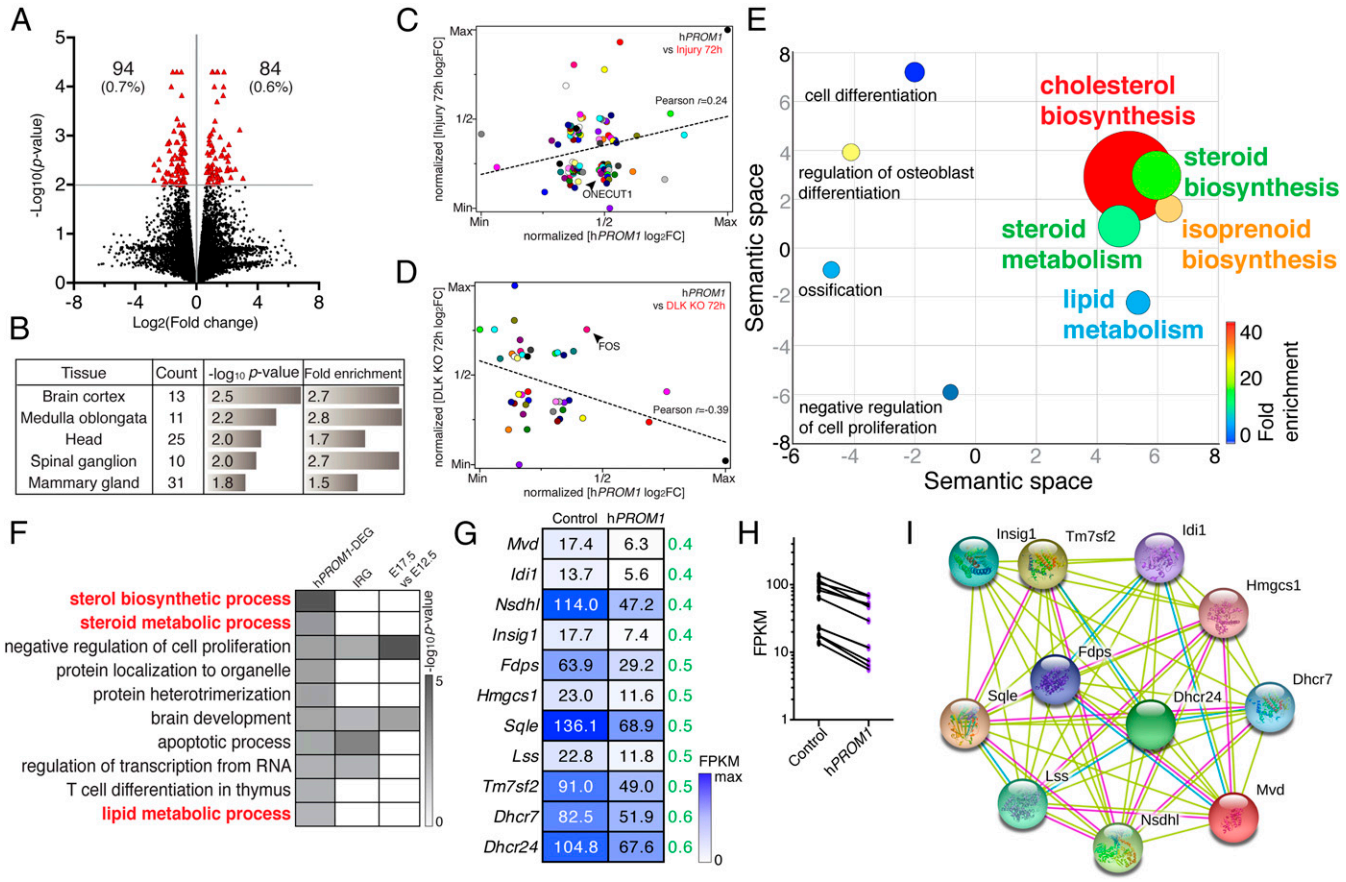

Fig. 5. *Prom1* regulates the expression of cholesterol metabolic genes in DRG neurons. (*A*) Differential gene expression presented as a volcano plot with the −log10 *P* value plotted against the log2 FC (*Prom1*-overexpressing neurons/control neurons). Transcripts with an FPKM value >0.1 and statistical significance defined by Cuffdiff were plotted (13,858 genes). The detection significance threshold was set to $P < 0.01$. A total of 94 genes were significantly down-regulated and 84 genes were significantly up-regulated by *Prom1* overexpression. (*B*) Tissue distribution of the identified DEGs known to be highly expressed using DAVID analysis. (*C* and *D*) The genes differentially regulated by h*PROM1* overexpression ($P < 0.05$) were compared with the previously reported injury-regulated, DLK-dependent DEG dataset identified in DRG tissue (3). For the DEGs listed in both datasets, log2-FC induced by nerve injury (at 72 h after sciatic nerve injury/uninjured control) are plotted against the log2-FC induced by *PROM1* overexpression (*PROM1*-overexpressing neurons/control neurons) in *C*. Log2-FC induced by DLK deficiency in injured neurons (at 72 h after injury, WT vs. *DLK*-KO) are plotted against the log2-FC induced by *PROM1* overexpression (*PROM1*-overexpressing neurons/control neurons) in *D*. (*E*) Biological pathways overrepresented in the *PROM1*-DEGs identified by DAVID GO analysis visualized using REVIGO. The circle diameter reflects the −log10-*P* value. The rainbow lookup table (LUT) of the color pallets indicates the fold enrichment scores between 0 and 40. (*F*) Comparative analysis of GO terms enriched from DEGs due to *PROM1* overexpression (h*PROM1*-DEG), from IRGs at 72 h after nerve injury vs. uninjured (3), and from developmentally regulated genes (E17.5 vs. E12.5) (6). The gray LUT indicates the inverse of the log10 *P* value from GO analysis. The white box indicates no statistical significance. (*G*) The 11 *PROM1*-DEGs associated with highly overrepresented biological processes (cholesterol biosynthesis, steroid biosynthesis, and steroid metabolism in *E*; FDR < 0.01) are listed with their adjusted FPKM values from the control and *PROM1*-overexpressing samples. The level is indicated by the blue LUT set from an RGB of (0,0,0) to RGB (0,0,255). The green numbers indicate the relative expression levels of the individual genes in *PROM1*-overexpressing cultures, normalized to those in control cultures. (*H*) Line plot showing the expression levels of the 11 *PROM1*-DEGs presented in *G*. All the genes were down-regulated by *PROM1* overexpression. (*I*) STRING analysis results indicating the functional association of the 11 *PROM1*-DEGs presented in *G*, supported by experimental reports (red line), curated databases (dark-green line), and text mining (light-green line). Refer to *SI Appendix*, Fig. S3.

that the selected DEGs indeed interact with each other in the lipid metabolic pathway. The DEGs were functionally related in the identical metabolic pathway based on proven experimental data or reported in the literature (Fig. 5*I* and Dataset S3) (66, 67). Therefore, the informatic analysis clearly indicates that *PROM1* specifically down-regulates the expression of cholesterol metabolism-associated genes, which might consequently inhibit lipid metabolism in the sterol synthesis pathway.

***PROM1* Regulates Cholesterol Metabolism through the Smad-Pathway.** Comparative analysis of the transcriptomes revealed that *PROM1* regulates the defined targets and suggested that cholesterol metabolism is potentially a cellular physiological process that can be manipulated to potentiate neuronal regeneration. To test this hypothesis, we first tested the cellular cholesterol level from the DRG neurons using a filipin staining assay (68, 69) and found that the cholesterol level is significantly reduced by *PROM1* overexpression (Fig. 6 *A* and *B*), indicating that the transcriptional down-regulation of the cholesterol metabolism genes by *PROM1* overexpression results in a reduction in neuronal cholesterol. We then investigated whether the regenerative potential could be directly changed by manipulating neuronal cholesterol levels. Elevation of cellular cholesterol levels with water-soluble cholesterol (Fig. 6*A*) significantly reduced axonal regrowth (Fig. 6 *C* and *D*). The neurons were also characterized by an unusual morphology when cellular cholesterol levels were elevated, with a number of filopodium-like structures with F-actin observed around the cell body (Fig. 6*A*). In contrast, the depletion of cholesterol using methyl-β-cyclodextrin (MβCD) (Fig. 6*A*) promoted the regenerative

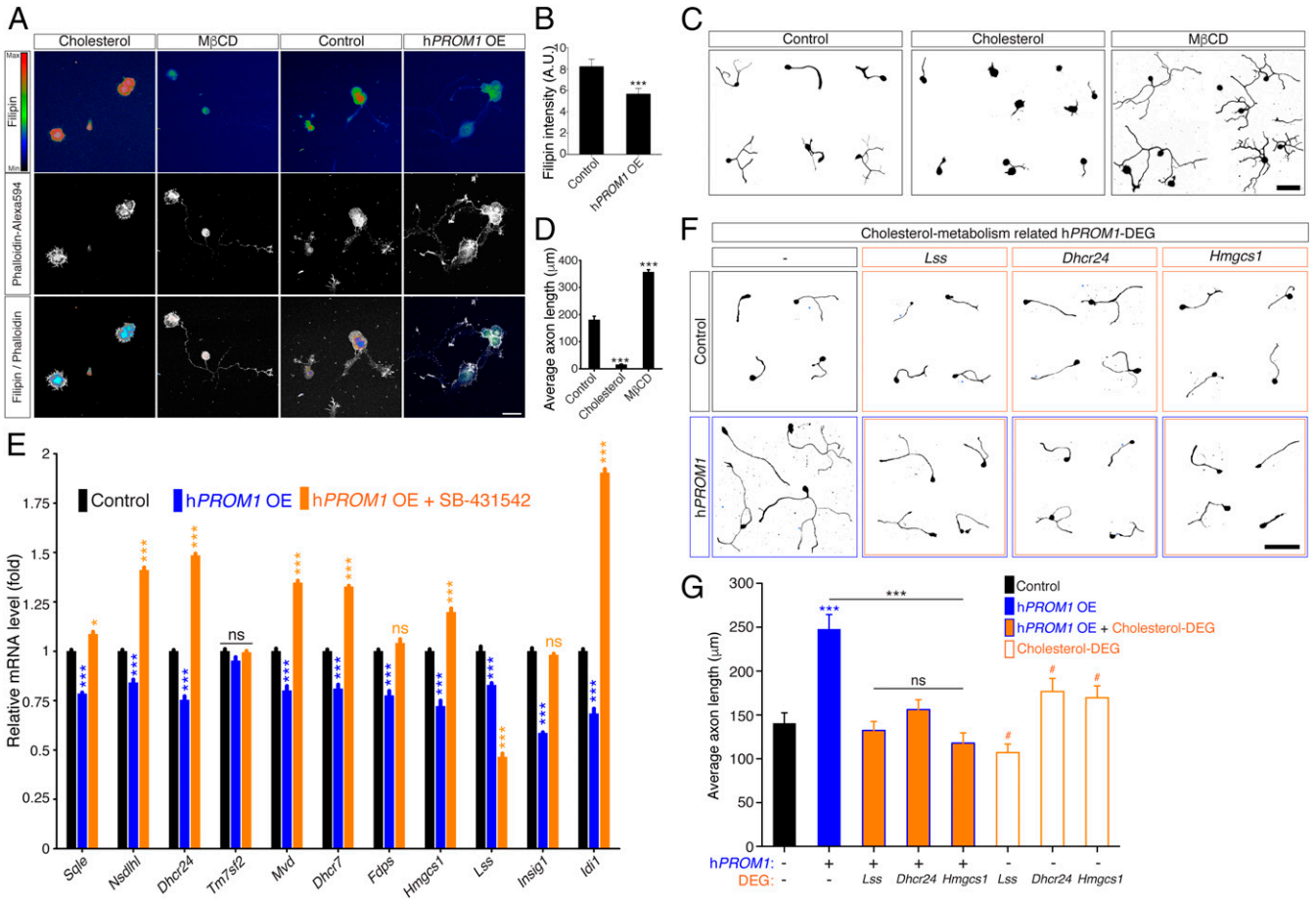

Fig. 6. *Prom1* reduces cellular cholesterol levels to promote axon regeneration. (*A*) Representative images of the replated embryonic DRG neurons costained by filipin for cholesterol and phalloidin for F-actin. Cultured embryonic DRG neurons were transduced with a control or *PROM1*-overexpressing lentivirus at DIV2, replated at DIV5, and fixed and stained after 12 h. Treatment with MβCD or water-soluble cholesterol at replating is shown as a control. (Scale bar: 100 μm.) Raw fluorescent intensity of filipin staining was transformed to rainbow color-LUT using ImageJ with RGB code from black (0,0,0) to red (255,0,0) to visualize the intensity. (*B*) Results from *A* were quantified for the filipin III staining intensity level. Data are mean ± SEM. (*C*) In vitro axon regeneration assays with cholesterol or MβCD. Cultured embryonic DRG neurons were replated at DIV5 and incubated with water-soluble cholesterol (50 μM) or MβCD (500 μM). Representative images are collected together in a single panel for each experimental condition. (Scale bar: 100 μm.) (*D*) Average length of axons from *C*. Data are mean ± SEM. (*E*) RT-qPCR analysis of expression levels of the DEGs listed in Fig. 5*G*. RNA from control or *Prom1*-overexpressing embryonic DRG neurons (vehicle-treated or 1 μM SB-431542–treated) was subjected to qPCR analysis. Data are mean ± SEM. (*F*) In vitro regeneration assay of *PROM1*-expressing neurons with individual coexpression of *Lss*, *Dhcr24*, and *Hmgcs1*, which are *PROM1*-DEGs down-regulated by *PROM1* overexpression. Embryonic DRG neurons were transduced by lentivirus for overexpression and subjected to replating assays. (Scale bar: 100 μm.) (*G*) The average length of axons from *F*. Data are mean ± SEM. Refer to *SI Appendix*, Figs. S4 to S7.

potential, with the DRG neurons producing elongated axons with an extensively branched structure (Fig. 6 *C* and *D*).

A recent study also reported that cholesterol depletion by nystatin enhances both CNS and PNS nerve regeneration (70). Thus, we further tested whether manipulating cholesterol levels alters the axon growth phenotype observed in the *PROM1* depletion and overexpression models. Water-soluble cholesterol treatment inhibited the improvement of axon regeneration in the adult DRG neurons cultured from mice injected with AAV-h*PROM1* and preconditioned by injury, with reducing average axon length to the control (AAV-GFP) level or further down in a dose-dependent manner (*SI Appendix*, Fig. S4). In addition, treating MβCD to adult DRG neurons cultured from *Prom1* KO mice rescued the impaired axon regeneration observed after conditioning injury (*SI Appendix*, Fig. S5). Applying MβCD did not increase axonal growth after replating in the regeneration-promoting condition with DLK overexpression, further suggesting that the cholesterol metabolism is specifically involved in regenerative axon outgrowth (*SI Appendix*, Fig. S6). Collectively, these data suggest that cellular cholesterol levels are functionally involved in the *Prom1*-mediated regulation of axon regeneration.

Because TGF-β/Smad signaling is known to transcriptionally down-regulate cholesterol metabolism genes, such as *Srebp*, *Nrf2*, *Dhcr24*, *Dhcr7*, *Hmgcs1*, and *Sqle* (71), we tested the requirement of Smad-pathway for *Prom1*-mediated transcriptional regulation using SB-431542 to inhibit TGF-β signaling. We found that pharmacologic inhibition of the Smad pathway mostly restored the expression levels of the cholesterol metabolism DEGs down-regulated by *PROM1* overexpression (Fig. 6*E*). We also investigated other *PROM1*-DEGs with functional annotations that were overrepresented in the *PROM1*-dependent transcriptome, such as differentiation. *Trib1*, *Sema6a*, and *Smarca2* were selected and tested with in vitro regeneration assay (Dataset S4). We found that knocking down *Trib1* or *Sema6a* had no effect on regenerative potential, as assessed by replating assays, and only knocking down *Smarca2* inhibited axonal regrowth after replating (*SI Appendix*, Fig. S7). These results suggest that cholesterol metabolism-related pathways are the primary physiological processes regulated by *PROM1* in potentiating the neuronal

regenerative program. Consistently, improved axonal regrowth by *PROM1* overexpression was inhibited by coexpressing the cholesterol metabolism-associated *PROM1*-DEGs *Lss*, *Dhcr24*, and *Hmgcs1* in replating assays using embryonic DRG neurons (Fig. 6 *F* and *G*). Expressing the individual *PROM1*-DEGs alone did not alter axonal regrowth. Collectively, these results demonstrate that *PROM1* functions as a negative regulator of cholesterol metabolism by downregulating the expression of defined target genes, resulting in potentiation of the neuroregenerative process through the Smad-dependent signaling pathway.

***Prom1* Is Required for Axonal Injury-Induced Smad Signaling.** Because *PROM1*-mediated transcriptional regulation is mediated by the Smad pathway, we investigated whether injury-induced activation of Smad signaling requires *Prom1*. We examined Smad2 phosphorylation from the DRG in vivo and found that basal levels of phosphorylated Smad2 (p-Smad2) were significantly reduced in the DRG neurons from *Prom1* KO mice (Fig. 7 *A* and *B*). Moreover, nuclear accumulation of p-Smad2 after injury was significantly impaired in the *Prom1* KO mice (Fig. 7*A*), supporting the requirement of *Prom1* for the Smad-dependent transcriptional changes triggered by nerve injury. Although Smad activation in non-neuronal cells inhibits axon regeneration by inducing scar formation in the damaged spinal cord (72, 73), the neuronal Smad-signaling is one of the major signal transduction pathways promoting regeneration (74).

Because *Prom1* is required for neuronal activation of the Smad2 pathway, we determined whether *PROM1*-dependent promotion of the regenerative potential is mediated by the Smad pathway. Indeed, we found that overexpression of *PROM1* up-regulated phosphorylation of Smad2 in cultured embryonic DRG neurons (Fig. 7*C*). In vivo, conditioning lesion and *Prom1* overexpression by AAV-h*PROM1* displayed an additive effect on activating Smad2 signaling as demonstrated by nuclear localization of p-Smad2 (*SI Appendix*, Fig. S8). Furthermore, blocking of Smad signaling by SB-431542 treatment significantly impaired the enhancement of axon regeneration observed in adult DRG neurons cultured from mice injected with AAV-h*PROM1* (Fig. 7 *D–F*).

Finally, the involvement of Smad2 signaling provides a testable hypothesis for the mechanisms by which the transmembrane protein prominin-1 regulates transcription. Smad2 was previously reported to mediate a signaling cascade activated by activin, which is a TGF-β superfamily ligand and determinant of axon regeneration capacity (5, 75). Activin binds to a type I TGF-β receptor, ALK4, which is inhibited by SB-431542. Thus, we hypothesized that prominin-1 can interact with ALK4 and modulate activin signaling to subsequently activate Smad2 and regulate transcription. Indeed, immunoprecipitation experiments showed that prominin-1 binds to ALK4 (Fig. 7*G*). Furthermore, coexpression of prominin-1 and hALK4 had a synergistic effect on phosphorylating Smad2 for its activation in HEK293T cells (Fig. 7*H*). The activation of Smad2 signaling by *Prom1* is dependent on the localization of *Prom1* on the plasma membrane, because treatment of LS-7 blocks the increase in p-Smad2 by *PROM1* overexpression in embryonic DRG neurons in vitro (*SI Appendix*, Fig. S9). Taken together, these results indicate that *Prom1* is a key molecular mediator activating injury-induced

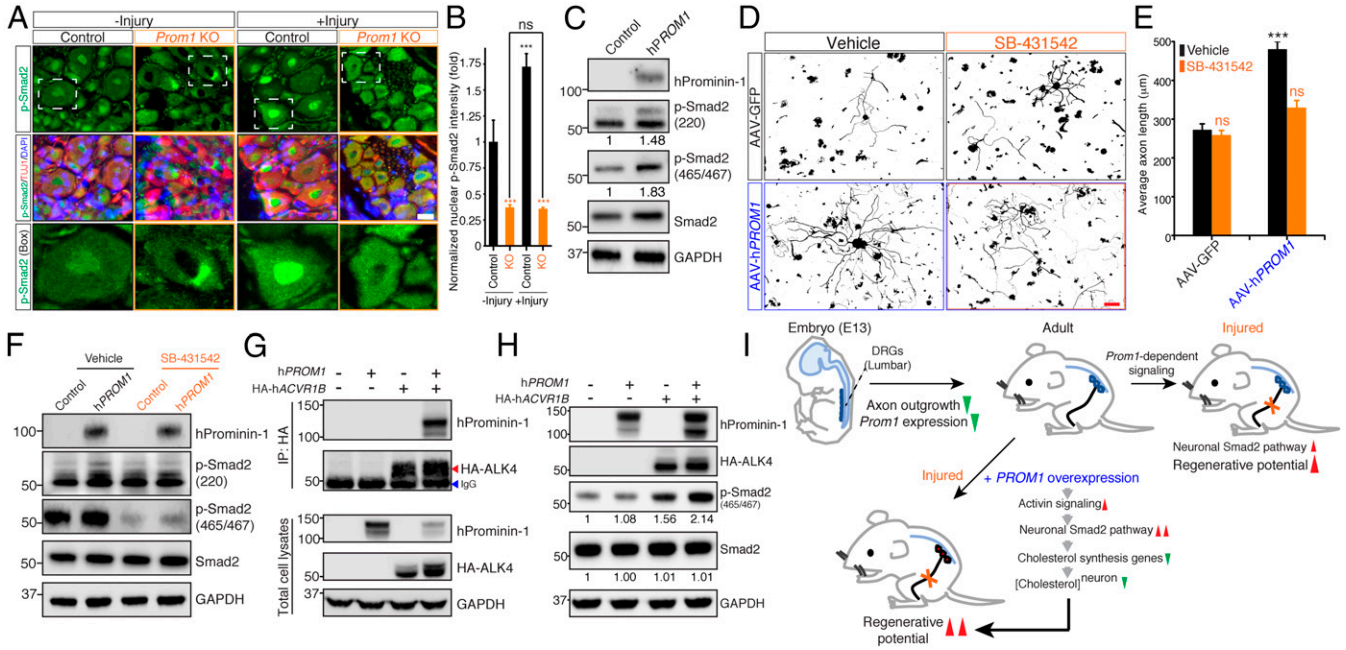

Fig. 7. *Prom1* is required for injury-responsive Smad signaling activating the regenerative potential. (*A*) Representative DRG sections stained with p-Smad2, βIII tubulin, and DAPI. The mouse L4-5 DRG tissues were dissected at 24 h after sciatic nerve injury (+Injury) from control or *Prom1*-KO mice. (Scale bar: 50 μm.) (*B*) Relative levels of fluorescence intensity of the nuclear p-Smad2 normalized to the total p-Smad2 signal. Data are mean ± SEM. (*C*) Western blot analysis of p-Smad2 levels in protein extracts prepared from control or *PROM1*-expressing embryonic DRG neurons. The numbers indicate the relative intensity obtained from ImageStudio (LI-COR). (*D*) Adult DRG neurons dissected from preconditioned AAV-GFP or AAV-h*PROM1* mice at 3 d after sciatic nerve injury. The neurons were plated and incubated with vehicle or SB-431542. (Scale bar: 100 μm.) (*E*) The average length of axons from *D*. Data are mean ± SEM. (*F*) Western blot analysis of p-Smad2 levels in protein extracts prepared from control or *PROM1*-expressing embryonic DRG neurons with or without SB-431542 treatment. Anti-human prominin-1 antibody was used to confirm expression of h*PROM1*. (*G*) Immunoprecipitation assay result demonstrating the interaction between human prominin-1 and ALK4 (*ACVR1B*; activin receptor type-1B). HA-ALK4 protein was immunoprecipitated by anti-HA antibody and analyzed by Western blot analysis to detect coprecipitated human prominin-1. (*H*) Western blot analysis of p-Smad2 overexpressing h*PROM1* with or without HA-ALK4. The numbers indicate the relative intensity obtained from ImageStudio (LI-COR). (*I*) Schematic diagram of the *PROM1*-dependent regulation of axon regeneration potential. *Prom1* expression levels decline across the developmental stages. In adults, preconditioning by axonal injury activates the neuron-intrinsic regeneration program. *Prom1* is required for activation of Smad2-signaling during preconditioning, and increasing the neuronal *PROM1* level enhances the regenerative ability in injured DRG neurons via Smad-dependent down-regulation of cholesterol synthesis genes. Refer to *SI Appendix*, Figs. S8 and S9.

Smad signaling, and that *Prom1* promotes the regenerative potential in injured neurons via Smad signaling that transcriptionally regulates cholesterol metabolism (Fig. 7*I*).

Discussion

The present study shows that *Prom1* is a neuron-intrinsic regulator of axon regeneration in injured PNS neurons, and that *Prom1* overexpression reduces the expression of specific genes involved in cholesterol metabolism by the Smad pathway, leading to enhancement of the regenerative response in injured neurons. Our data strongly suggest that the in vivo gene delivery of *PROM1* has the potential to promote regenerative potential in injured neurons. The regenerative potential is lower in adult neurons than during their development (34). The neuronal transition from the extending stage to the transmitting phase during development is supported by the expression of genes that suppress axonal growth in the late developmental stages (6). Based on this, we hypothesized that the developmental decline of regenerative ability may be caused by the down-regulation of growth-promoting genes, such as those associated with stemness. An analysis of developmental transcriptome data revealed that a set of stem cell marker genes is down-regulated as neurons mature. Of these, prominin-1 is still expressed at low levels in DRG neurons in adult mice. This observation led us to test whether the developmental decline of *Prom1* expression is linked to the loss of robust axon regeneration in adults and to consider the possible role of *Prom1* in regeneration in the mature PNS (20, 34, 76–78).

We found that *Prom1* is required for efficient axon regeneration in PNS neurons in vitro and in vivo. *Prom1* promotes axon regrowth after injury by inducing neuronal regenerative states. *Prom1* overexpression induces activation of Smad2 and leads to an increase in regrown axonal length on CSPGs, inhibitory substrates found in the nonpermissive environment of damaged CNS tissue. We further identified 178 *PROM1*-DEGs and found that the genes regulated by *PROM1* overexpression partially overlap our previously published list of injury-responsive genes with DLK dependency, supporting the involvement of *PROM1* in the transcriptional regeneration program. Notably, we found that most of the down-regulated *PROM1*-DEGs share a common cellular pathway regulating cholesterol synthesis, as revealed by GO and *STRING* analysis, and that the down-regulation is mediated by Smad signaling. Indeed, *PROM1* overexpression reduced cellular cholesterol levels, which potentiates axon regeneration. Smad signaling is responsible for the axon regeneration enhancement induced by *PROM1* overexpression and we show that *Prom1* regulates Smad signaling via interaction with ALK4, the type I TGF-β receptor. Finally, we found that the AAV-mediated gene delivery of *PROM1* promotes axon regeneration in vivo in adult mice. Moreover, with in vitro assays that can distinguish responses in naïve neurons vs. preconditioned neurons, we found that AAV-mediated expression of *PROM1* is not sufficiently effective for promoting axonal regrowth in naïve neurons. Instead, *PROM1* overexpression potentiates the regenerative output stimulated by nerve injury in a synergistic manner. Studies using the spinal cord injury model should be conducted to examine the effect of *Prom1* overexpression on improving axon regeneration in injured CNS axons.

Prominin-1 is known to bind to cholesterol (79), but the biological role of prominin-1 remains unclear. Prominin-1 has been proposed to regulate membrane topology and promote the formation of filopodia-like protrusions (80). In addition, prominin-1 is known to be responsible for the regulation of tunneling nanotubes, the F-actin–based plasma membrane channels that bridge the gaps between cells (81). Thus, it has been suggested that prominin-1 functions within the cellular membrane and is involved in the regulation of interface mediating cellular communication. This function might be related to the active reorganization of the axonal membrane during axon regeneration. There has been no evidence supporting the role of prominin-1 as a molecular receptor, as biological ligands interacting with the extracellular region of prominin-1 has not been reported. However, our data using LS-7, the putative inhibitor of prominin-1, suggest that the *Prom1*-induced potentiation of regeneration may depend on the receptor function of prominin-1. Alternatively, the interaction of LS-7 with the extracellular regions might induce structural changes in prominin-1, leading to inhibition of its molecular function in promoting regenerative potential. Importantly, our biochemical data indicate that prominin-1 interacts with ALK4, an activin receptor, supporting a role of prominin-1 in modulating the activin signaling-dependent potentiation of axon regeneration. These possibilities should be investigated in the future by identifying biomolecules that potentially regulate prominin-1 functions, allowing the development of applications that promote axon regeneration regulated by prominin-1–associated mechanisms. The role of cholesterol in localizing prominin-1 in particular domains of the plasma membrane also remains to be studied in the regenerative signaling, because treating MβCD to deplete cellular cholesterol led to the complete inhibition of the *PROM1* overexpression effect (*SI Appendix*, Fig. S6). In addition, it will be an interesting future direction to study the possible non–cell-autonomous *Prom1* function for regulating axon regeneration from the vascular structure near the DRG cell bodies, where strong expression of *Prom1* was detected.

Preconditioning requires transcriptomic regulation, which changes the physiological condition of neurons from a naïve state to a regenerative state (60). Although the mechanisms underlying this process are not yet fully understood, it has been proven that the disorganization of the cytoskeleton, such as microtubule disruption by nocodazole, induces regeneration-associated signal transduction and potentiates regenerative capacity (57). In addition, a series of reports has shown that administering cytoskeleton-reorganizing chemicals, such as Taxol and epothilone B, promotes axon regeneration in vivo (72, 73). Therefore, injury-induced cytoskeletal disorganization may play a pivotal role in regulating the regenerative potential.

We found that prominin-1 down-regulates the expression of the genes involved in cholesterol metabolism, which subsequently reduces cellular cholesterol levels. It is known that plasma membrane cholesterol levels control cellular physical properties and morphology, including protruding structures, through cytoskeletal reorganization (82, 83). Consistently, our data show that the neurons treated with MβCD display extensively arborized neurites with a dramatic increase in axon growth length, although it is distinguished from the characteristic axon elongation in the regenerative phase, possibly due to the overall depletion of cholesterol from different cellular domains. Collectively, the data suggest that prominin-1 plays a role in modulating cellular architecture by regulating the expression of cholesterol metabolism-related genes, shifting the physiological condition from a naïve state to a regenerative state, which leads to enhanced axon regeneration after injury. A recent report by Hori and colleagues (84) showed that *Prom1* overexpression induced cell membrane extensions at the rear edge of the moving RPE1 cells, a human immortalized retinal pigmented epithelium-derived cell line. The induced fibers are rich in cholesterol, seemingly in conflict with our observation that *Prom1* overexpression leads to down-regulation of cholesterol. The two studies describe distinct mechanistic bases—the small GTPase-dependent fiber formation vs. Smad-dependent transcriptional down-regulation of cholesterol synthesis genes—and the cell types examined (i.e., epithelial cells and neurons, respectively) might contribute to the different outcomes. Alternatively, it is also possible that despite lower total cytoplasmic cholesterol levels, *Prom1* overexpression leads to a local increase in cholesterol concentration in specific foci. It should be studied in the future to identify a mechanistic link between cholesterol levels and efficiency of axon extension. Moreover, investigating

the mechanisms by which prominin-1 induces the transcriptional regulation of the specific set of target genes is an important future research direction.

Our findings aid the understanding of neuroregeneration. First, we identify cholesterol metabolism as a neuronal physiological target for the manipulation of regenerative potential. Lipid metabolism has recently been implicated in the regulation of injured optic nerve regeneration, suggesting the balance between triglycerides and phospholipids as a determinant of neuronal regenerative capacity in the CNS (85). Likewise, a recent study by Roselló-Busquets and colleagues (70) suggested manipulating cholesterol levels as an approach to improve axon regeneration in the PNS. The present study strengthens the evidence supporting the therapeutic strategy based on cholesterol metabolism, and also contributing to improved mechanistic understanding. We suggest that activin-ALK4-Smad2 signaling is a pathway that can modulate cholesterol levels in injured neurons when sufficiently activated, as by *Prom1* overexpression. Cholesterol metabolism is known to be related to brain development and neurologic disease, and because of its clinical association with cardiovascular disease, various drugs have been actively used to manipulate cholesterol levels in patients (86). These drugs may be potential candidates for neuroregeneration and functional recovery and merit investigation in this respect.

Second, therapeutic applications may need to consider that the regenerative potential can be manipulated by stemness-related molecules. Additional stem cell markers with previously unknown functions are worth considering as candidates for promoting the regenerative potential.

Finally, our study suggests that neuronal cholesterol levels can be an effective biomarker for monitoring the physiological conditions of neurons, including their regenerative potential. There is no practical way to determine the naïve, regenerative, and degenerative states of neurons before they enter into an irreversible biological cascade. This is a serious hurdle for the development of approaches to ensure neuronal survival and regeneration before the initiation of axonal destruction and neuronal death. Our findings provide a basis for the design of a method for assessing neuronal conditions based on the monitoring of cholesterol metabolism and its associated gene expression. Importantly, our biochemical data show that prominin-1 interacts with ALK4, an activin receptor, supporting a role of prominin-1 in modulating the activin signaling-dependent potentiation of axon regeneration. These possibilities should be investigated in the future by identifying biomolecules that potentially regulate prominin-1 functions, allowing the development of applications that promote axon regeneration regulated by prominin-1–associated mechanisms.

Materials and Methods

Adult DRG Cell Culture and Replating Assay. All animal husbandry and surgical procedures were approved by Korea University Institutional Animal Care & Use Committee. Surgeries were performed under isoflurane anesthesia following the regulatory protocols. To monitor the neuronal regenerative potential, DRG tissues located at L4 and L5 were dissected from adult mice treated with or without preconditioning at 3 d before the dissection. DRG neurons were cultured as described previously (27). In brief, the DRG tissues were serially incubated in DMEM/Liberase TM (Roche; 5401119001)/DNase I (Sigma-Aldrich; DN25)/BSA and trypsin-EDTA for 15 min each at 37 °C and followed by trituration. Dissociated cells were plated in DMEM/10% FBS/1% penicillin-streptomycin/1% Glutamax (Thermo Fisher Scientific; 35050-061) on four-well Lab-Tek chamber slides (Thermo Fisher Scientific; 177437) coated with poly-D-lysine (Sigma-Aldrich; P0899) and laminin (Invitrogen; 23017-015) and incubated in humidified 37 °C, 5% CO_2 incubator. To introduce an inhibitory substrate of axonal growth, the neurons were plated on the substrate coated with chondroitin sulfate proteoglycans (Merck; CC117; 1 μg/mL). For in vitro replating assay, the cultured DRG neurons were trypsinized for 5 min and replated on new culture plates at 3 d after the initial plating. The replated neurons were fixed and immunostained with anti-βIII tubulin antibody at 12 h after replating. Axon regeneration was quantified by measuring the longest axonal length per neuron from the βIII tubulin-stained images. Regeneration potential was assessed by the average axon length and cumulative percentage for axonal length.

Embryonic DRG Cell Culture and Replating Assay. Embryonic DRG cultures were generated as described previously (27). Embryonic DRG collected from E13.5 mice were dissociated in 0.05% trypsin-EDTA and plated on poly-D-lysine/laminin–coated dishes in Neurobasal medium (Gibco) supplemented with 2% B-27 (Gibco), 1% Glutamax, 1 μM 5-fluoro-2′-deoxyuridine (Sigma-Aldrich), 1 μM uridine (Sigma-Aldrich), 1% penicillin-streptomycin, and 50 ng/mL 2.5S nerve growth factor (Envigo; BT-5017). For lentiviral transduction, lentivirus was added to the culture at DIV2. For the replating assay using embryonic DRG cultures, neurons were replated at DIV5. In brief, cultures were incubated in DMEM/0.05% Trypsin-EDTA mixture (1:1) for 5 min at 37 °C, 5% CO_2 and rinsed with culture medium described above. Cells were then dissociated by gentle pipetting and transferred to new culture plates coated with poly-D-lysine/laminin. Replated neurons were incubated overnight at 37 °C with 5% CO_2. Neurite lengths were measured and assessed as described above for the adult neuronal replating assay. Chondroitin sulfate proteoglycans (1 μg/mL) were mixed in the laminin coating solution for assays on the inhibitory substrate. To reduce cellular cholesterol levels, 0.5 mM MβCD (Sigma-Aldrich; C4555) was applied to cultures. To increase cholesterol levels, cells were treated with 50 μM water-soluble cholesterol (Sigma-Aldrich; C4951) at replating. SB-431542 was purchased from Tocris (1614) and used at 1 μM.

LS-7 Treatment and Binding Assay. LS-7, the heptameric peptide (amino acid sequence: LQNAPRS) screened by Sun and colleagues (59) was synthesized with fluorescein (FITC) conjugation from Peptron (Daejeon, Korea). The HEK293T cell line used for the LS-7 peptide-binding assay was cultured in medium containing 10% FBS (HyClone) and 100 U/mL penicillin/streptomycin in DMEM (HyClone; sh30243.01) at 37 °C with 5% CO_2. To express *PROM1* in HEK293T cells, the plasmid encoding *PROM1* was transfected by Lipofectamine2000 (Thermo Fisher Scientific; 11668-019) according to the manufacturer's instructions. The cells were incubated in 180 nM LS-7–FITC or vehicle-containing fresh culture medium for 2 h at 24 h after transfection and then fixed in 4% paraformaldehyde for 15 min at room temperature. The cells were washed with one culture volume of PBS and then subjected to immunocytochemistry analysis. Detailed descriptions of the methodology are provided in *SI Appendix*.

Data Availability. The RNA-seq data have been deposited to the Gene Expression Omnibus (GEO) database (accession no. GSE147936).

ACKNOWLEDGMENTS. This work was supported by the National Research Foundation of Korea funded by the Korean Ministry of Science, Information and Communication Technology and Future Planning (Grants 2015R1A5A1009024, to Y.C. and S.W.C and 2016R1A5A2007009, to J.E.S.).

1. National Institutes of Health, Appendix E: Stem Cell Markers. https://stemcells.nih.gov/info/2001report/appendixE.htm. Accessed 23 July 2009.
2. A. Tedeschi, P. G. Popovich, The application of omics technologies to study axon regeneration and CNS repair. *F1000 Res.* **8**, F1000 Faculty Rev-311 (2019).
3. J. E. Shin, H. Ha, Y. K. Kim, Y. Cho, A. DiAntonio, DLK regulates a distinctive transcriptional regeneration program after peripheral nerve injury. *Neurobiol. Dis.* **127**, 178–192 (2019).
4. J. E. Shin, H. Ha, E. H. Cho, Y. K. Kim, Y. Cho, Comparative analysis of the transcriptome of injured nerve segments reveals spatiotemporal responses to neural damage in mice. *J. Comp. Neurol.* **526**, 1195–1208 (2018).
5. V. Chandran *et al.*, A systems-level analysis of the peripheral nerve intrinsic axonal growth program. *Neuron* **89**, 956–970 (2016).
6. A. Tedeschi *et al.*, The calcium channel subunit Alpha2delta2 suppresses axon regeneration in the adult CNS. *Neuron* **92**, 419–434 (2016).
7. K. K. Park *et al.*, Promoting axon regeneration in the adult CNS by modulation of the PTEN/mTOR pathway. *Science* **322**, 963–966 (2008).
8. K. Liu *et al.*, PTEN deletion enhances the regenerative ability of adult corticospinal neurons. *Nat. Neurosci.* **13**, 1075–1081 (2010).
9. P. Nix, N. Hisamoto, K. Matsumoto, M. Bastiani, Axon regeneration requires coordinate activation of p38 and JNK MAPK pathways. *Proc. Natl. Acad. Sci. U.S.A.* **108**, 10738–10743 (2011).
10. K. Ben-Yaakov *et al.*, Axonal transcription factors signal retrogradely in lesioned peripheral nerve. *EMBO J.* **31**, 1350–1363 (2012).
11. J. E. Shin *et al.*, Dual leucine zipper kinase is required for retrograde injury signaling and axonal regeneration. *Neuron* **74**, 1015–1022 (2012).
12. F. Sun *et al.*, Sustained axon regeneration induced by co-deletion of PTEN and SOCS3. *Nature* **480**, 372–375 (2011).

13. S. Miraglia *et al*., A novel five-transmembrane hematopoietic stem cell antigen: Isolation, characterization, and molecular cloning. *Blood* **90**, 5013–5021 (1997).
14. A.H. Yin *et al*., AC133, a novel marker for human hematopoietic stem and progenitor cells. *Blood* **90**, 5002–5012 (1997).
15. A. Weigmann, D. Corbeil, A. Hellwig, W. B. Huttner, Prominin, a novel microvilli-specific polytopic membrane protein of the apical surface of epithelial cells, is targeted to plasmalemmal protrusions of non-epithelial cells. *Proc. Natl. Acad. Sci. U.S.A.* **94**, 12425–12430 (1997).
16. S. Zacchigna *et al*., Loss of the cholesterol-binding protein prominin-1/CD133 causes disk dysmorphogenesis and photoreceptor degeneration. *J. Neurosci.* **29**, 2297–2308 (2009).
17. J. Permanyer *et al*., Autosomal recessive retinitis pigmentosa with early macular affectation caused by premature truncation in PROM1. *Invest. Ophthalmol. Vis. Sci.* **51**, 2656–2663 (2010).
18. T. L. Walker *et al*., Prominin-1 allows prospective isolation of neural stem cells from the adult murine hippocampus. *J. Neurosci.* **33**, 3010–3024 (2013).
19. K. Nishide, Y. Nakatani, H. Kiyonari, T. Kondo, Glioblastoma formation from cell population depleted of Prominin1-expressing cells. *PLoS One* **4**, e6869 (2009).
20. Z. Li, CD133: A stem cell biomarker and beyond. *Exp. Hematol. Oncol.* **2**, 17 (2013).
21. M. Curcio, F. Bradke, Axon regeneration in the central nervous system: Facing the challenges from the inside. *Annu. Rev. Cell Dev. Biol.* **34**, 495–521 (2018).
22. M. T. Filbin, Myelin-associated inhibitors of axonal regeneration in the adult mammalian CNS. *Nat. Rev. Neurosci.* **4**, 703–713 (2003).
23. Z. He, Y. Jin, Intrinsic control of axon regeneration. *Neuron* **90**, 437–451 (2016).
24. M. Mahar, V. Cavalli, Intrinsic mechanisms of neuronal axon regeneration. *Nat. Rev. Neurosci.* **19**, 323–337 (2018).
25. E.-M. Hur *et al*., Engineering neuronal growth cones to promote axon regeneration over inhibitory molecules. *Proc. Natl. Acad. Sci. U.S.A.* **108**, 5057–5062 (2011).
26. R. Puttagunta *et al*., PCAF-dependent epigenetic changes promote axonal regeneration in the central nervous system. *Nat. Commun.* **5**, 3527 (2014).
27. Y. Cho, R. Sloutsky, K. M. Naegle, V. Cavalli, Injury-induced HDAC5 nuclear export is essential for axon regeneration. *Cell* **155**, 894–908 (2013).
28. R. Lindner, R. Puttagunta, S. Di Giovanni, Epigenetic regulation of axon outgrowth and regeneration in CNS injury: The first steps forward. *Neurotherapeutics* **10**, 771–781 (2013).
29. J. E. Shin, Y. Cho, Epigenetic regulation of axon regeneration after neural injury. *Mol. Cells* **40**, 10–16 (2017).
30. Y. Cho, V. Cavalli, HDAC signaling in neuronal development and axon regeneration. *Curr. Opin. Neurobiol.* **27**, 118–126 (2014).
31. T. H. Hutson *et al*., Cbp-dependent histone acetylation mediates axon regeneration induced by environmental enrichment in rodent spinal cord injury models. *Sci. Transl. Med.* **11**, eaaw2064 (2019).
32. F. M. Mar, A. Bonni, M. M. Sousa, Cell intrinsic control of axon regeneration. *EMBO Rep.* **15**, 254–263 (2014).
33. I. Palmisano, S. Di Giovanni, Advances and limitations of current epigenetic studies investigating mammalian axonal regeneration. *Neurotherapeutics* **15**, 529–540 (2018).
34. J. Cai, M. L. Weiss, M. S. Rao, In search of "stemness". *Exp. Hematol.* **32**, 585–598 (2004).
35. C. T. Maguire *et al*., Genome-wide analysis reveals the unique stem cell identity of human amniocytes. *PLoS One* **8**, e53372 (2013).
36. M. Perycz, A. S. Urbanska, P. S. Krawczyk, K. Parobczak, J. Jaworski, Zipcode binding protein 1 regulates the development of dendritic arbors in hippocampal neurons. *J. Neurosci.* **31**, 5271–5285 (2011).
37. R. Dutton, T. Yamada, A. Turnley, P. F. Bartlett, M. Murphy, Sonic hedgehog promotes neuronal differentiation of murine spinal cord precursors and collaborates with neurotrophin 3 to induce Islet-1. *J. Neurosci.* **19**, 2601–2608 (1999).
38. F. Renaud *et al*., The neurotrophic activity of fibroblast growth factor 1 (FGF1) depends on endogenous FGF1 expression and is independent of the mitogen-activated protein kinase cascade pathway. *J. Biol. Chem.* **271**, 2801–2811 (1996).
39. D. Singer *et al*., Prominin-1 controls stem cell activation by orchestrating ciliary dynamics. *EMBO J.* **38**, e99845 (2019).
40. D. Corbeil, K. Röper, C. A. Fargeas, A. Joester, W. B. Huttner, Prominin: A story of cholesterol, plasma membrane protrusions and human pathology. *Traffic* **2**, 82–91 (2001).
41. D. Corbeil, A. M. Marzesco, M. Wilsch-Bräuninger, W. B. Huttner, The intriguing links between prominin-1 (CD133), cholesterol-based membrane microdomains, remodeling of apical plasma membrane protrusions, extracellular membrane particles, and (neuro)epithelial cell differentiation. *FEBS Lett.* **584**, 1659–1664 (2010).
42. G. S.-L. Peh, R. J. Lang, M. F. Pera, S. M. Hawes, CD133 expression by neural progenitors derived from human embryonic stem cells and its use for their prospective isolation. *Stem Cells Dev.* **18**, 269–282 (2009).
43. C. V. Pfenninger *et al*., CD133 is not present on neurogenic astrocytes in the adult subventricular zone, but on embryonic neural stem cells, ependymal cells, and glioblastoma cells. *Cancer Res.* **67**, 5727–5736 (2007).
44. S. El Hallani *et al*., A new alternative mechanism in glioblastoma vascularization: Tubular vasculogenic mimicry. *Brain* **133**, 973–982 (2010).
45. R. Wang *et al*., Glioblastoma stem-like cells give rise to tumour endothelium. *Nature* **468**, 829–833 (2010).
46. A. Adini *et al*., The stem cell marker prominin-1/CD133 interacts with vascular endothelial growth factor and potentiates its action. *Angiogenesis* **16**, 405–416 (2013).
47. M. Florek *et al*., Prominin-1/CD133, a neural and hematopoietic stem cell marker, is expressed in adult human differentiated cells and certain types of kidney cancer. *Cell Tissue Res.* **319**, 15–26 (2005).
48. C. V. Pfenninger *et al*., CD133 is not present on neurogenic astrocytes in the adult subventricular zone, but on embryonic neural stem cells, ependymal cells, and glioblastoma cells. *Cancer Res.* **67**, 5727–5736 (2007).
49. G. S.-L. Peh, R. J. Lang, M. F. Pera, S. M. Hawes, CD133 expression by neural progenitors derived from human embryonic stem cells and its use for their prospective isolation. *Stem Cells Dev.* **18**, 269–282 (2009).
50. A. Lee *et al*., Isolation of neural stem cells from the postnatal cerebellum. *Nat. Neurosci.* **8**, 723–729 (2005).
51. L. Zhu *et al*., Prominin 1 marks intestinal stem cells that are susceptible to neoplastic transformation. *Nature* **457**, 603–607 (2009).
52. G. Yiu, Z. He, Glial inhibition of CNS axon regeneration. *Nat. Rev. Neurosci.* **7**, 617–627 (2006).
53. E. J. Bradbury *et al*., Chondroitinase ABC promotes functional recovery after spinal cord injury. *Nature* **416**, 636–640 (2002).
54. L. D. F. Moon, R. A. Asher, K. E. Rhodes, J. W. Fawcett, Regeneration of CNS axons back to their target following treatment of adult rat brain with chondroitinase ABC. *Nat. Neurosci.* **4**, 465–466 (2001).
55. R. J. McKeon, M. J. Jurynec, C. R. Buck, The chondroitin sulfate proteoglycans neurocan and phosphacan are expressed by reactive astrocytes in the chronic CNS glial scar. *J. Neurosci.* **19**, 10778–10788 (1999).
56. A. Tedeschi, F. Bradke, Spatial and temporal arrangement of neuronal intrinsic and extrinsic mechanisms controlling axon regeneration. *Curr. Opin. Neurobiol.* **42**, 118–127 (2017).
57. V. Valakh, E. Frey, E. Babetto, L. J. Walker, A. DiAntonio, Cytoskeletal disruption activates the DLK/JNK pathway, which promotes axonal regeneration and mimics a preconditioning injury. *Neurobiol. Dis.* **77**, 13–25 (2015).
58. E. Frey, S. Karney-Grobe, T. Krolak, J. Milbrandt, A. DiAntonio, TRPV1 agonist, capsaicin, induces axon outgrowth after injury via Ca^{2+}/PKA signaling. *eNeuro* **5**, ENEURO.0095-18.2018 (2018).
59. J. Sun *et al*., A novel mouse CD133-binding peptide screened by phage display inhibits cancer cell motility in vitro. *Clin. Exp. Metastasis* **29**, 185–196 (2012).
60. D. S. Smith, J. H. Skene, A transcription-dependent switch controls competence of adult neurons for distinct modes of axon growth. *J. Neurosci.* **17**, 646–658 (1997).
61. G. Quadrato, S. Di Giovanni, Waking up the sleepers: Shared transcriptional pathways in axonal regeneration and neurogenesis. *Cell. Mol. Life Sci.* **70**, 993–1007 (2013).
62. J. Lee *et al*., PROM1(CD133)-dependent expressed genes from mouse embryonic DRG neurons. Gene Expression Omnibus. https://www.ncbi.nlm.nih.gov/geo/query/acc.cgi?acc=GSE147936. Deposited 1 April 2020.
63. T. C. Ma, D. E. Willis, What makes a RAG regeneration associated? *Front. Mol. Neurosci.* **8**, 43 (2015).
64. M. J. Finelli, K. J. Murphy, L. Chen, H. Zou, Differential phosphorylation of Smad1 integrates BMP and neurotrophin pathways through Erk/Dusp in axon development. *Cell Rep.* **3**, 1592–1606 (2013).
65. F. Supek, M. Bošnjak, N. Škunca, T. Šmuc, REVIGO summarizes and visualizes long lists of gene ontology terms. *PLoS One* **6**, e21800 (2011).
66. D. Szklarczyk *et al*., STRING v11: Protein-protein association networks with increased coverage, supporting functional discovery in genome-wide experimental datasets. *Nucleic Acids Res.* **47**, D607–D613 (2019).
67. T. J. Tracey, F. J. Steyn, E. J. Wolvetang, S. T. Ngo, Neuronal lipid metabolism: Multiple pathways driving functional outcomes in health and disease. *Front. Mol. Neurosci.* **11**, 10 (2018).
68. H. Zhang *et al*., Intracellular cholesterol biosynthesis in enchondroma and chondrosarcoma. *JCI Insight* **5**, 127232 (2019).
69. I. de Diego *et al*., Cholesterol modulates the membrane binding and intracellular distribution of annexin 6. *J. Biol. Chem.* **277**, 32187–32194 (2002).
70. C. Roselló-Busquets *et al*., Cholesterol depletion regulates axonal growth and enhances central and peripheral nerve regeneration. *Front. Cell. Neurosci.* **13**, 40 (2019).
71. C. Coulouarn, V. M. Factor, S. S. Thorgeirsson, Transforming growth factor-β gene expression signature in mouse hepatocytes predicts clinical outcome in human cancer. *Hepatology* **47**, 2059–2067 (2008).
72. F. Hellal *et al*., Microtubule stabilization reduces scarring and causes axon regeneration after spinal cord injury. *Science* **181**, 928–931 (2011).
73. J. Ruschel *et al*., Systemic administration of epothilone B promotes axon regeneration after spinal cord injury. *Science* **348**, 347–352 (2015).
74. J. Zhong, H. Zou, BMP signaling in axon regeneration. *Curr. Opin. Neurobiol.* **27**, 127–134 (2014).
75. T. Omura *et al*., Robust axonal regeneration occurs in the injured CAST/Ei mouse CNS. *Neuron* **86**, 1215–1227 (2015).
76. C. E. Adler, A. Sánchez Alvarado, Types or states? Cellular dynamics and regenerative potential. *Trends Cell Biol.* **25**, 687–696 (2015).
77. M. Bilodeau, G. Sauvageau, Uncovering stemness. *Nat. Cell Biol.* **8**, 1048–1049 (2006).
78. X. Lan *et al*., CD133 silencing inhibits stemness properties and enhances chemoradiosensitivity in CD133-positive liver cancer stem cells. *Int. J. Mol. Med.* **31**, 315–324 (2013).
79. K. Röper, D. Corbeil, W. B. Huttner, Retention of prominin in microvilli reveals distinct cholesterol-based lipid micro-domains in the apical plasma membrane. *Nat. Cell Biol.* **2**, 582–592 (2000).
80. D. Corbeil, K. Röper, M. J. Hannah, A. Hellwig, W. B. Huttner, Selective localization of the polytopic membrane protein prominin in microvilli of epithelial cells—a combination of apical sorting and retention in plasma membrane protrusions. *J. Cell Sci.* **112**, 1023–1033 (1999).
81. D. Reichert *et al*., Tunneling nanotubes mediate the transfer of stem cell marker CD133 between hematopoietic progenitor cells. *Exp. Hematol.* **44**, 1092–1112.e2 (2016).
82. M. Sun *et al*., The effect of cellular cholesterol on membrane-cytoskeleton adhesion. *J. Cell Sci.* **120**, 2223–2231 (2007).
83. N. Khatibzadeh, A. A. Spector, W. E. Brownell, B. Anvari, Effects of plasma membrane cholesterol level and cytoskeleton F-actin on cell protrusion mechanics. *PLoS One* **8**, e57147 (2013).
84. A. Hori *et al*., Prominin-1 modulates Rho/ROCK-mediated membrane morphology and calcium-dependent intracellular chloride flux. *Sci. Rep.* **9**, 15911 (2019).
85. C. Yang *et al*., Rewiring neuronal glycerolipid metabolism determines the extent of axon regeneration. *Neuron* **105**, 276–292.e5 (2020).
86. P. J. Barter, K. Rye, New era of lipid-lowering drugs. *Pharmacol. Rev.* **68**, 458–475 (2016).